AD-A176 362 INVESTIGATION OF CE(3+) DOPANT IN APPROPRIATE HOSTS FOR BLUE GREEN LASERS(U) CRYSTAL SYSTEMS INC SALEM MA C P KHATTAK 25 NOV 86 CSI-86-120 N00014-82-C-0747 F/G 20/5 1/1 NL

UNCLASSIFIED

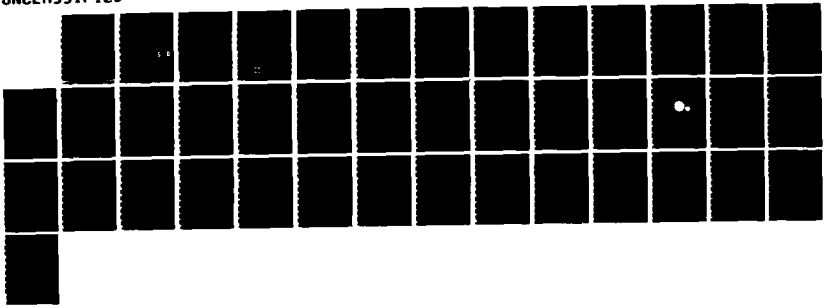

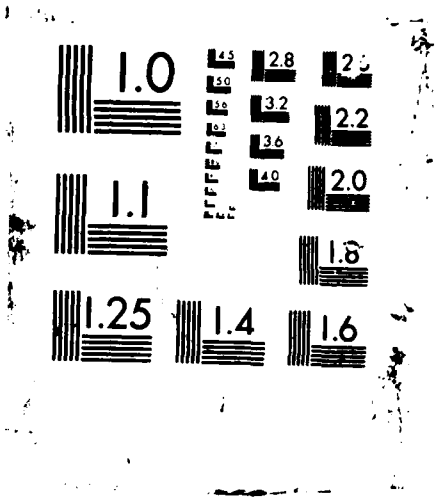
1.0
1.1
1.25
1.4
1.6
2.8
3.2
3.6
4.0
2.2
2.0
1.8

(12)

SECURITY CLASSIFICATION OF THIS PAGE (When Data Entered)

REPORT DOCUMENTATION PAGE		READ INSTRUCTIONS BEFORE COMPLETING FORM
1. REPORT NUMBER N00014-82-C-0747	2. GOVT ACCESSION NO.	3. RECIPIENT'S CATALOG NUMBER
4. TITLE (and Subtitle) INVESTIGATION OF Ce^{3+} DOPANT IN APPROPRIATE HOSTS FOR BLUE GREEN LASERS		5. TYPE OF REPORT & PERIOD COVERED FINAL Report covering period 9/1/82 - 7/31/85 6. PERFORMING ORG. REPORT NUMBER
7. AUTHOR(s) Chandra P. Khattak		8. CONTRACT OR GRANT NUMBER(s) N00014-82-C-0747
9. PERFORMING ORGANIZATION NAME AND ADDRESS Crystal Systems, Inc. 27 Congress Street Salem, MA 01970		10. PROGRAM ELEMENT, PROJECT, TASK AREA & WORK UNIT NUMBERS Program Element #61153N Proj.Task Area RR011-07-04 Work Unit #NR379-057
11. CONTROLLING OFFICE NAME AND ADDRESS Office of Naval Research (Code 1112) 800 Quincy Street Arlington, VA 22217		12. REPORT DATE 11/25/86 13. NUMBER OF PAGES
14. MONITORING AGENCY NAME & ADDRESS(if different from Controlling Office) -		15. SECURITY CLASS. (of this report) Unclassified 15a. DECLASSIFICATION/DOWNGRADING SCHEDULE

16. DISTRIBUTION STATEMENT (of this Report)

Approved for public release; distribution unlimited.

17. DISTRIBUTION STATEMENT (of the abstract entered in Block 20, if different from Report)

Approved for public release; distribution unlimited.

18. SUPPLEMENTARY NOTES

19. KEY WORDS (Continue on reverse side if necessary and identify by block number)

solid-state laser
underwater communication
Cd doped
$LaAlO_3$
$Ce:Gd_3Sc_2Al_3O_{12}$
$Pr:KMgY_3F_{12}$
$La(Al_{0.75}Sc_{0.25})O_3$
$(La_{0.98}Ba_{0.02})(Al_{0.98}Zr_{0.02})O_3$
$(La_{0.98}Sr_{0.02})(Al_{0.98}Zr_{0.02})O_3$
Gd_2SiO_5
La_2SiO_5

20. ABSTRACT (Continue on reverse side if necessary and identify by block number)

Blue green lasers are required for communication under sea water. Currently, no solid-state laser shows inherent fluorescence in the blue green spectrum. Preliminary data at ONR had shown that Ce:$LaAlO_3$ offers promise for communication under sea water. $LaAlO_3$ exhibits a phase transformation at 435°C which creates problems in growing high quality crystals. Initial emphasis of the program was on making suitable additions to the $LaAlO_3$ in order to achieve a cubic perovskite structure which eliminates the phase transition. A composition of (please turn page over)

DD FORM 1 JAN 73 1473 EDITION OF 1 NOV 65 IS OBSOLETE
S/N 0102-LF-014-6601

SECURITY CLASSIFICATION OF THIS PAGE (When Data Entered)

Block 22 continued.

$La(Al_{0.75}Sc_{0.25})O_3$ was identified as cubic; however, high quality crystals could not be grown because of difficult crystal growth parameters which could not be obtained with available equipment. Two other compositions - $(La_{0.98}Ba_{0.02})(Al_{0.98}Zr_{0.02})O_3$ and $(LA_{0.98}Sr_{0.02})(Al_{0.98}Zr_{0.02})O_3$ - were also produced with cubic structure. Since Ba containing compound may exhibit quenching of fluorescence, the Sr compound may be useful for solid state laser applications. These bluish-green crystals are not expected to show flu escence in the blue-green spectral region.

In order to develop other crystals with lower melting point, an effort was also placed on $Ce:Gd_2SiO_5$, $Ce:La_2SiO_5$ and $Pr:KMgY_3F_{12}$. These samples were delivered to ONR for evaluation of fluorescence.

$Ce:Gd_3Sc_2Al_3O_{12}$ (Ce:GSAG) crystals were also grown by HEM. These crystals offer promise for solid state laser applications; however, it is necessary to grow improved quality crystals for evaluation of laser performance.

CSI Report No. 86-120

INVESTIGATION OF Ce^{3+} DOPANT IN APPROPRIATE HOSTS FOR BLUE GREEN LASERS

Final Report
ONR Contract No. N00014-82-C-0747
Covering period September 1, 1982 - July 31, 1985

Principal Investigator - C. P. Khattak
Program Manager - F. Schmid

Prepared for
DEPARTMENT OF THE NAVY
Office of Naval Research
Arlington, Virginia 22217

Report Issued: November 25, 1986

CRYSTAL SYSTEMS INC.
35 CONGRESS STREET
SALEM, MASSACHUSETTS 01970
(617) 745-0088 TWX 710 347 1523

Table of Contents

List of Figures

List of Tables

INVESTIGATION OF Ce^{3+} DOPANT IN APPROPRIATE HOSTS FOR BLUE-GREEN LASERS

1.0 Introduction

Underwater communication can be achieved with solid state laser sources in the blue-green spectral region. The wave length of most interest for these laser sources should be centered at ~ 480 nm. Therefore, crystals exhibiting blue-green luminescence are of considerable interest as solid state lasers. Ce^{3+}:$Y_3Al_5O_{12}$ (YAG) exhibits a broad luminescence centered around 520 nm[1,2] based upon the Ce^{3+} d → f luminescent transition[3]. This emission in Ce^{3+}:YAG is at too low energy and, therefore, precludes laser action[4]. The Ce^{3+} in YAG occupies the center of the cube of oxygen ions. In lattices such as $ScBO_3$ where Ce^{3+} is in octaheatal coordination with oxygen ions, the emission is typically observed at wavelengths less than 420 nm[2]. These symmetry-sensitive luminescence spectra are in keeping with the crystal field theory.

Based on the above considerations, luminescence was expected from Ce^{3+} centered at approximately 480 nm when the host lattice incorporated Ce^{3+} in a cubic symmetry with the oxygen in 8-fold coordination. In view of this, it was desirable to develop an appropriate host lattice for a blue-green laser using Ce^{3+} as the dopant.

The perovskite system appears to be an appropriate choice as an oxide host lattice. In this system $LaAlO_3$ appears to be an appropriate choice because of its large band gap, strong crystal field, and high thermal conductivity. However, the phase transition[5] at 435°C has presented considerable problems in trying to grow it in single crystal form. Therefore, additions to $LaAlO_3$ have to be made so as to suppress the phase transitions and, therefore, be able to grow single crystals. Some indication

of blue-green luminescence in Ce^{3+} doped $La(Al,Sc)O_3$ has been observed[6]; however, this sample was not well characterized.

During initial stages of the present program, efforts were made to study the feasibility of Ce^{3+}:$La(Al,Sc)O_3$ crystal growth by the Heat Exchanger Method (HEM™). After initial experiments, emphasis was placed on evaluating different materials which could be used as hosts for Ce^{3+}. A number of different hosts were formed which showed luminescence at wave lengths other than 480 nm or showed non-cubic symmetry so that large crystals could not be grown. Some of the compositions were identified which showed cubic symmetry. However, large single crystals could not be grown because of very stringent requirements for crystal growth, such as high temperatures of approximately 2200°C, high pressure to prevent volatilization and neutral/reducing atmosphere to retain Ce^{3+}, etc. Even though solid state laser crystals which show luminescence in the blue-green spectral region were not grown, a number of materials were identified which could be grown in single crystal form for laser applications.

2.0 Heat Exchanger Method (HEM™)

The Heat Exchanger Method (HEM) is being used for commercial production of sapphire and silicon crystals[7,8] and has been adapted for the growth of a number of solid state laser crystals[9,10] The salient features of the process are shown in Figure 1. The crucible with the seed positioned at the bottom is loaded with charge and placed on top of the heat exchanger. After evacuation, heat is supplied by the graphite heater and the charge is melted. The seed is prevented from melting by forcing gaseous helium through the heat exchanger.

After sufficient meltback of the seed is achieved, growth is started by increasing the flow of helium and thereby decreasing the heat exchanger temperature. The liquid temperature gradients are controlled by the furnace temperature while the temperature gradient in the solid is controlled by the heat exchanger temperature. Crystal growth is achieved by controlling the heat input as well as the heat extraction. After solidification is complete, the gas flow through the heat exchanger is decreased to equilibrate the temperature throughout the crystal during the annealing and cooldown stage.

HEM is the only crystal growth process in which independent liquid and solid temperature gradients are achieved without movement of the crucible, heat zone or crystal. After the crystal is grown, it is still in the heat zone and can be cooled at a controlled rate to relieve solidification stresses. This unique capability allowed the growth of sapphire up to 32 cm diameter and weighing about 50 kg without cracking due to thermal stresses associated with such large sizes.

A distinguishing feature of the HEM, as compared with Czochralski (Cz) or top-seeded processes, is that the solid-liquid interface is submerged beneath the surface and is surrounded by the melt. Under these conditions the thermal and mechanical perturbations are damped out by the surrounding molten mass before they reach interface. This results in uniform

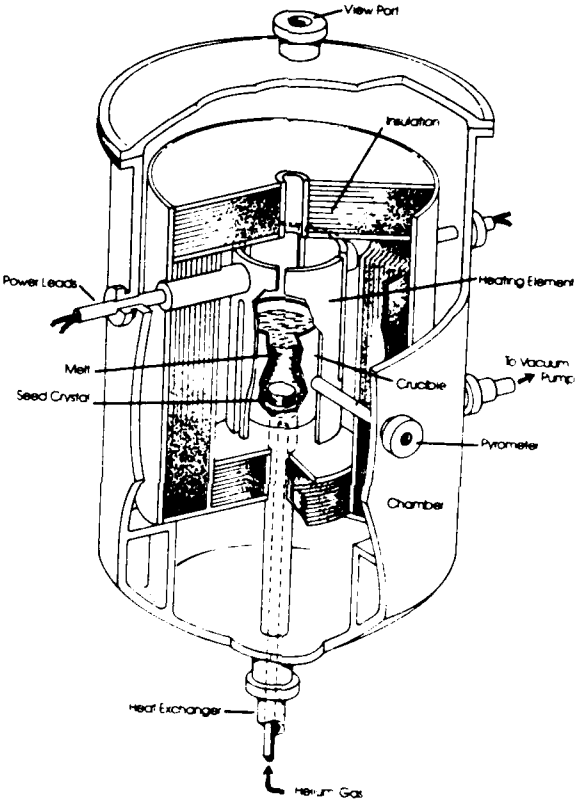

Figure 3. Schematic of HEM Furnace.

temperature gradients at the interface; consequently, neither the crystal nor the crucible is rotated. In the Cz process growth occurs at the melt surface where the local gradients vary sufficiently to cause solidification and remelting of the crystal. These features of HEM produce uniform growth and the only sapphire which is free of light scatter.

In the HEM growth, after the crystal is grown, the temperature of the furnace is reduced to just below the solidification temperature and the helium flow is reduced at a desired rate. The whole crystal can therefore be brought to high temperatures to anneal the solidification stresses and is then cooled uniformly at the controlled rate. Because *in situ* annealing is part of the solidification cycle, HEM can reduce the defect density. Further, the last and most impure material to solidify is along the crucible walls, where it can be removed.

In the case of sapphire and silicon, it was demonstrated that once crystal growth parameters are established, large crystals can be grown.

The HEM is currently being adapted for the growth of $Ti:Al_2O_3$, $Gd_3Sc_2Al_3O_{12}$ (GSAG), GaAs, CdTe, $Co:MgF_2$, aluminum oxynitride (ALON) and BaF_2 crystals.

From an economic point of view, HEM is a low-cost process. The furnace is automated and well insulated, which results in low labor and low energy costs.

3.0 Experimental Results

The objective of the program was to develop an appropriate host lattice for the Ce^{3+} dopant ion in order to produce blue-green luminescence which could be utilized for communication through sea water. During the initial stages of the program, emphasis was placed on perovskite oxides.

Simple perovskites can be identified as ABO_3 type compounds. $LaAlO_3$ appeared to be an appropriate choice because of its desirable properties. The phase transition at 435°C presented problems in growing this material in single crystal form. Suitable ions were substituted for Al in the B site in order to suppress the phase transition. In later stages, substitutions were also made for La in the A site. While these substitutions were made with trivalent ions, it was observed that the dopant Ce ion could easily go into tetravalent state because of non-stoichiometry of the oxygen sites. Substitutions were also made with divalent ions in the A site and tetravalent ions in the B site. Toward the end of the experimental phase, host lattices other than the perovskite, such as garnets, A_2SiO_5 type compounds and fluoride systems, were also evaluated. The details of the experiments carried out during the experimental stage are described in Table I. Samples were provided to the Office of Naval Research and the fluorescence data was obtained at the Naval Research Laboratory. The discussion for each system evaluated is written below.

3.1 Ce^{3+};$La(Al,Sc)O_3$ as Host Lattice

3.1.1 Choice of This System

Rare earths have found their widest application in optically-pumped solid-state lasers. Of the approximately 200 crystalline lasers reported, all are based upon rare earths except for a few iron group ions and one actinide ion.

Ce^{3+} has been shown[3] to exhibit 5d → 4f luminescent transition and therefore has potential for a solid state blue-

Table I. Details of Experimental Data

RUN NO.	CHARGE COMPOSITION	CHARGE WT. (gm)	MELT TEMP.	SUPER-HEAT	SOLIDIFICATION TIME (Hr)	COMMENTS
1	(LaO.8Sc0.2)AlO3	37.79	2095	25		
2	La(Al0.8Sc0.2)O3	44.40				
3	La(Al0.8Sc0.2)O3	39.40	2105	15	87	
4	LaAlO3	142.70	2105	10	144	Yellow on top, black on bottom.
5	La(Al0.8Sc0.2)O3	136.45	2040	30	112	Opaque.
6	La(Al0.8Sc0.2)O3	70.25	2055	60	145	Opaque. Air fired at 1200C.
7	La(Al0.8Sc0.2)O3	65.30	2110 max		136	Charge boiled out of crucible.
8	La(Al0.8Sc0.2)O3	75.85	2040 max			Held at 2040 for 36 hrs and cooled-charge melted. Air fired at 1200C.
9	La(Al0.8Sc0.2)O3	56.50	2120 max		148	Dark, opaque. Charge from Run #8.
10	La(Al0.7Sc0.3)O3	62.45	2115 max		99	Opaque. Material observed outside crucible.
11	La(Al0.7Sc0.3)O3	61.15	2060	35	28	Light yellow translucent on top. Opaque, black on bottom.
12	La(Al1-xScx)O3	36.25				3 crucibles loaded into furnace. Solid state synthesis, no melting.
13	La(Al0.5Sc0.5)O3	29.05	2060	20	111	Yellow on top, black on bottom.
14	La(Al0.8Sc0.2)O3	35.65	2050	30	67	Mat'l from 12A. Single phase, rhombohedral. Yellow to black.

Table I. Details of Experimental Data

RUN NO.	CHARGE COMPOSITION	CHARGE WT. (gm)	MELT TEMP.	SUPER-HEAT	SOLIDIFICATION TIME (Hr)	COMMENTS
15	La(Al0.5Sc0.5)O3	19.95	2060	30	66	Mat'l. synthesized in 12C opaque.
16	La(Al0.7Sc0.3)O3	26.25	2040	40	114	'Mat'l. from 12B two phase.
17	La(Al0.75Sc0.25)O3	35.40	2040	50	136	Semi-translucent. Yellow top single phase.
18	La(Al0.8Sc0.2)O3	53.40	2065	30	112	Translucent, lt. green bottom. opaque top.
19	La(Al0.75Sc0.25)O3	38.15	2060	40	142	Darker lower portion, light yellow top.
20	La(Al0.75Sc0.25)O3	90.70	2070	40	119	Several interfaces, some clear areas. Also black & yellow.
21	'a(Al0.75Sc0.25)O3	94.30	2070	40	182	Translucent center, opaque bottom.
22	La(Al0.75Sc0.25)O3	95.30	2075 max		119	Yellow, translucent top, opaque bottom.
23	La(Al0.75Sc0.25)O3	91.80	2060	0	141	Dark grey, crystalline. Operated under vacuum because of heating element problems.
24	LaAlO3	99.90	2075	25	88	Significant material loss.
25	LaAlO3	92.25	2075	25	74	Fragmented. Small grain size.

Table I. Details of Experimental Data

RUN NO.	CHARGE COMPOSITION	CHARGE WT. (gm)	MELT TEMP.	SUPER-HEAT	SOLIDIFICATION TIME (Hr)	COMMENTS
26	La(Al0.75Sc0.25)O3	16.70				Charge contained in isolated tungsten/moly chamber. inside furnace.
27	La(Al0.75Sc0.25)O3	16.70	2080 max		48	Same chamber as 26, same charge as 26. Charge melted, carbon contamination evident.
28	La(Al0.75Sc0.25)O3	29.35	2080 max		69	Melt not visible.
29	La(Al0.75Sc0.25)O3	34.80				Solid state synthesis, not melted. New isolated tungsten chamber.
30	La(Al0.33Sc0.66)O3	55.79				Solid state synthesis. Grey film on outside, white interior.
31	La(Al0.33Sc0.66)O3	50.79				White mat'l. from #30 ground & pressed. Sintering experiment.
32	La(Al0.33Sc0.66)O3	48.78	2080	20	42	Mat'l. from #31. White crystalline.
33	La(Al0.33Sc0.66)O3	40.94	2120 max		25	Mat'l. from #32. Melted.
34	(La0.5Gd0.5)ScO3	47.68				Blue, white,yellow. Sintered mass.
35	(La0.5Gd0.5)ScO3	40.80				Blue, white, yellow mass Sintered.
36	(La0.75Gd0.25)ScO3	22.17				Sintered. White.
37	(Ba0.5La0.5)Zr0.5Sc0.5)					

Table I. Details of Experimental Data

RUN NO.	CHARGE COMPOSITION	CHARGE WT. (gm)	MELT TEMP.	SUPER-HEAT	SOLIDIFICATION TIME (Hr)	COMMENTS
38	Gd(Sc0.5Al0.5)O3	24.12				Sintering experiment.
39	(LaAlO3)0.95(BaZrO3)0.05	21.93				Sintered. Majority phase-cubic.
40	(LaAlO3)0.5(BaZrO3).05	18.45				Multiphases.
41	BaZrO3	48.17	2145			Held at 80% power for 4 hrs and cooled.
42	(LaAlO3).95(BaZrO3).05	21.05	2120	5	40	Most mat'l. blue with green-yellow on o.d. Cubic symmetry.
43	Gd3Sc2Al3012	31.71	1880	20		Heat exchanger leak. Non-transparent crystallites. Blue-green fluorescence.
44	BaZrO3	47.85				Solid-state synthesis. White with brown speckles.
45	Gd3Sc2Al3012	63.55	1857	15	29	Crystals a few millimeters in size.
46	(LaAlO3)0.98(BaZrO3).02					Clean cubic.
47	(LaAlO3)0.5(SrZrO3)0.5	58.78				Solid-state synthesis. Outside black. core, brownish-yellow.
48	(LaAlO3)0.95(SrZrO3)0.05	22.22				Solid state synthesis. Substitute Sr for Ba to eliminate quenching.
49	(LaAlO3)0.95(SrZrO3)0.05	43.91				Solid state synthesis.
50	Gd2SiO5	42.26	1912	33		

Table I. Details of Experimental Data

RUN NO.	CHARGE COMPOSITION	CHARGE WT. (gm)	MELT TEMP.	SUPER-HEAT	SOLIDIFICATION TIME (Hr)	COMMENTS
51	La2SiO5	38.61				Solid state synthesis. La(OH)3 after standing in air.
49A	KMgYF#7	47.39	830	100	2	Sample from Airtron.
50A	KMgYF#7	52.29	930	55		Sample from Airtron. Lost power after melt. Sample cooled rapidly.
51A	KMgYF#7	50.71	1001 max			Remelt of #50/A. Several large crystallites.
52	Gd2SiO5	41.99	1382	63	4	Melted one phase. Ceramic appearance.
52A	Gd2SiO5	41.71	1900	60	7	Removed 52 from furnace and remelted.

green laser. The host material should have a large energy gap to lower-lying 4f states in order to prevent parasitic excited state absorption processes in the host conduction band. It is important to maintain Ce in trivalent state; the Ce^{4+} gives absorption. An oxide host lattice is desirable because of high thermal conductivity and strong crystal field. $LaAlO_3$ appears to be an appropriate choice as both La and Al are in trivalent state.

The perovskite $LaAlO_3$ has a rhombohedral structure[11] at room temperature. This material is in the $R\bar{3}m$ space group with lattice parameters a_o =5.357Å and α =60° 06′. The deviation from cubic symmetry is exhibited by the rhombohedral angle, α; for α =60° the material would show cubic symmetry[12]. $LaAlO_3$ transforms[5] to the cubic structure above 435°C. If large crystals of $LaAlO_3$ are grown, they are expected to exhibit cracking during the cooldown stage through this phase transformation. Suitable substitutions are, therefore, necessary in the Al sites to expand the lattice such that a cubic structure is formed. A review of the ionic radii of trivalent rate earth ions[13,15] shows that with the exception of the value for scandium, these ionic radii are quite large and, in fact, are among the largest values for any trivalent ions. Therefore, scandium ions could be substituted in the Al sites of $LaAlO_3$. In fact, $LaScO_3$ has been reported in literature[16]. The ionic sizes of Sc^{3+} and Al^{3+} are 0.83 and 0.57Å, respectively; Sc^{3+} substitution, therefore, would expand the $LaAlO_3$ lattice and tend towards cubic symmetry.

Ternary phase diagrams for La_2O_3-Al_2O_3-Sc_2O_3 are not known. However, binary phase diagrams exist. From the La_2O_3-Al_2O_3 phase diagram[17] (Figure 2) it can be seen that $LaAlO_3$ melts congruently at 2100°C. The Sc_2O_3-Al_2O_3 phase diagram[18] (Figure 3) shows that at about 20 mole % Sc_2O_3, a single phase solid solution phase is formed and the formation of α-Al_2O_3 is prevented. The range of this solid solution phase is ~ 18 to 35 mole % Sc_2O_3 at 1600 °C.

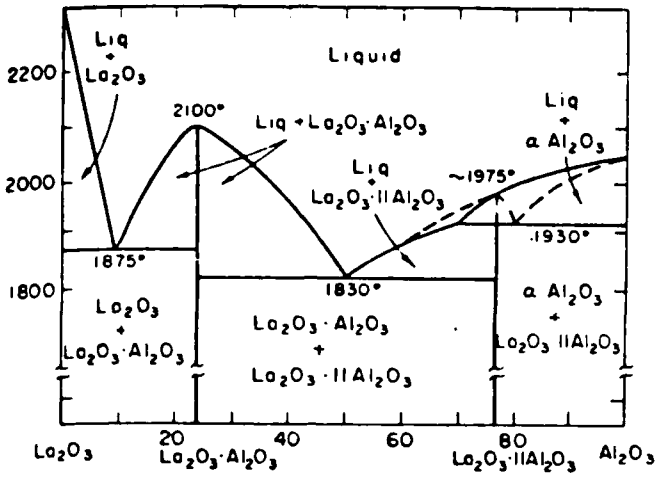

Figure 2. Phase Diagram for Al_2O_3-La_2O_3 System

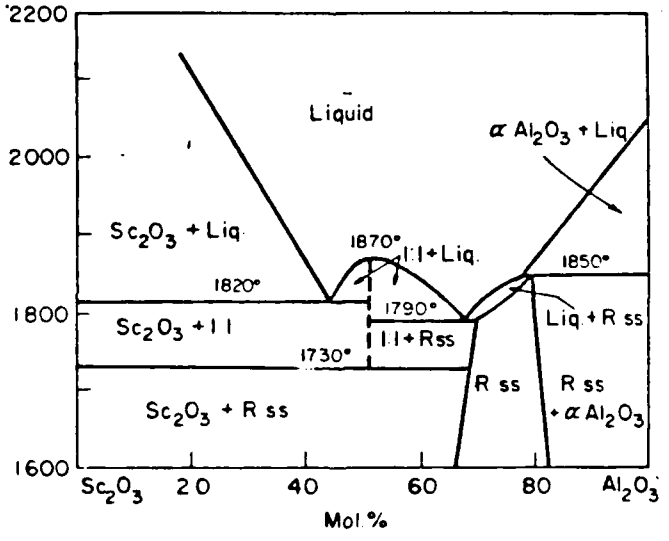

Figure 3. Phase Diagram for Al_2O_3-Sc_2O_3 System

From theoretical considerations, therefore, it appears that $La(Al,Sc)O_3$ crystals can be grown with a cubic structure. This material can then be used as a laser host material for Ce dopant ions. Trivalent Ce will substitute for La sites and compounds $CeAlO_3$ and $CeScO_3$ are reported in literature[19,20]. The amount of Ce substitution necessary for lasing action is expected to be about 0.02%.

Initial work sponsored by the Office of Naval Research was an attempt at growing a crystal of $La(Al_{0.8}Sc_{0.2})O_3$ doped with 0.01% Ce. During one experiment a small amount of the charge was fused in an iridium crucible. The experiment was aborted because of melting of the crucible. Optical spectra taken of the fused sample was characteristic of a cubic phase. The sample was rather inhomogeneous; however, it demonstrated that a cubic phase is formed in the $La(Al,Sc)O_3$ system and spectra show encouraging results for laser properties[6].

3.1.2 Crystal Growth of $La(Al,Sc)O_3$ by HEM

Initial work was carried out to evaluate the appropriate crucible and the atmosphere to be used for a $La(Al,Sc)O_3$ system. Since the ternary phase diagram is not known for this system, it is difficult to predict the various phases that can be formed in this system. It is essential to retain the dopant, Ce, in the trivalent state. Therefore, it is necessary to maintain a non-oxidizing atmosphere. Early work carried out under vacuum showed that the volatility of the phases formed resulted in a considerable loss of meltstock by evaporation. Further experiments were, therefore, under an argon atmosphere.

A molybdenum crucible was used which showed some reactivity with the charge at high temperatures. When molybdenum crucibles are used in vacuum, the volatile MoO_3 is removed; under argon atmosphere, this oxide is retained in the furnace chamber. Tungsten crucibles were found to be satisfactory.

Once the crucible and atmosphere were established, an attempt was made to grow $LaAlO_3$ crystals. The La_2O_3-Al_2O_3 phase

diagram is shown in Figure 2. No problems were encountered and a few mm size crystals were obtained. An x-ray diffraction pattern of crystals from Experiment #4 was taken and the pattern showed rhombohedral symmetry and could be indexed on the basis of hexagonal cell size of a=5.34 Å c=13.10Å. The observed and calculated 'd' values are shown in Table II. This data compares well with the published values[11,21] for $LaAlO_3$. An IRD-Guinier x-ray pattern was taken at Brookhaven National Laboratory and the pattern showed rhombohedral distortion of a cubic cell size of 3.8Å.

Experiments were carried out with a charge corresponding to $La(Al_{0.8}Sc_{0.2})O_3$. A molybdenum crucible was used and the lid on the crucible was held down with a weight placed on top of the cover. The material was taken up to 2120°C and slowly cooled. X-ray analysis of this data showed a two-phase structure for a sample from Experiment #3. Both the phases were rhombohedral distortion of the perovskite structure with lattice parameters of 3.86 Å and 3.99 Å, respectively. This data shows that the perovskite cell size has been enlarged from 3.8 Å with the substitution of Sc ions for the Al ions.

Another experiment was carried out with $La(Al_{0.8}Sc_{0.2})O_3$ charge composition. This time no cover was placed on the tungsten crucible. The resultant material (#5W) showed a single-phase, rhombohedral symmetry with perovskite cell size of 3.83 Å. The Laue pattern showed the single crystal nature of the material.

Since the phase diagram of the ternary system La_2O_3-Al_2O_3-Sc_2O_3 is not known, it is postulated that for the composition $La(Al_{0.8}Sc_{0.2})O_3$ two phases are formed. One of these phases is more volatile and during heating in the crucible without cover this phase volatilizes resulting in single-phase material. When a cover is placed on the crucible volatilization is minimized and two phases are formed. A review of the Al_2O_3-Sc_2O_3 binary phase diagram (Figure 2) shows that for 20 mole percent Sc_2O_3 substitution, a single phase is formed at high temperature;

TABLE II. Observed and calculated 'd' values of an x-ray diffraction pattern of $LaAlO_3$ based on hexagonal cell size of a=5.34 Å, c=13.10 Å

'd' values		hkl
Observed	Calculated	
3.79	3.78	012
2.67	2.67	110
2.28	2.28	021
2.18	2.18	006
1.89	1.89	024
1.73	1.73	211
1.69	1.69	122,116
1.54	1.54	300,214,018
1.339	1.336	208
1.339	1.335	220
1.260	1.260	306
1.190	1.195	128
1.190	1.194	134
1.140	1.140	0210,226,402
1.090	1.092	0012

however, a two-phase region exists at lower temperatures.

It was decided to pursue two approaches: first, to attempt solidification from a lower temperature with $La(Al_{0.8}Sc_{0.2})O_3$ composition to minimize volatilization; and second, to evaluate $La(Al_{0.7}Sc_{0.3})O_3$ composition.

An experiment was carried out in which $La(Al_{0.8}Sc_{0.2})O_3$ composition was heated to the 2020°C to 2040°C temperature range, held for about 36 hours and then cooled. No significant weight loss was observed and the boule (#8) after removal from the crucible is shown in Figure 4. Large crystallites are seen on the top surface. X-ray analysis of the ingot showed that it was not of rhombohedral symmetry, as was the case with other samples. The x-ray data could be indexed as a single-phase, orthorhombic structure with cell parameters a=5.08, b=5.65 and c=7.72 Å. A comparison of the observed and calculated d values is shown in Table III. The difference between the a and b lattice parameters appears large; the symmetry could be monoclinic. The perovskite unit cell is about 3.84 Å.

The material solidified under similar conditions in Experiment #10 using $La(Al_{0.7}Sc_{0.3})O_3$ showed a two-phase structure.

Work with the $La(Al,Sc)O_3$ system showed that, depending upon the composition as well as the experimental conditions, the symmetry was changed from rhombohedral to orthorhombic or monoclinic. During the stage when emphasis was placed on heating the material to well over 2100°C, significant weight loss was associated with each experiment. Once it was determined that with Sc substitutions the melting point of the compound was lower than the $LaAlO_3$, most of the experiments were carried out under low superheat conditions. Some of the compounds were analyzed after solid state synthesis to minimize volatilization from the melt. In Experiment #12, compounds of $La(Al_{1-x}Sc_x)O_3$ with x=0.2, 0.3 and 0.5 were heated to about 1700°C and cooled. X-ray diffraction data showed two phases for all the three compounds; one phase was closer to $LaAlO_3$ lattice parameter (~ 3.8 Å) and

Figure 4. A view of an ingot of $La(Al_{0.8}Sc_{0.2})O_3$ after HEM solidifcation

TABLE III. Observed and calculated 'd' values of an x-ray diffraction pattern of $La(Al_{0.8}Sc_{0.2})O_3$ based on orthorhombic cell size of a=5.08, b=5.65, c=7.72 Å

' d ' values		hkl
Observed	Calculated	
5.68	5.08	100
5.68	5.65	010
3.88	3.86	002
3.88	3.78	110
3.26	3.39	111
3.18	3.19	012
3.18	3.07	102
2.83	2.83	020
2.73	2.70	112
2.46	2.47	120
2.28	2.32	210
2.28	2.30	103
2.24	2.28	022
2.22	2.22	211
2.13	2.13	113
2.13	2.12	202
1.93	1.93	004
1.92	1.90	023
1.88	1.89	220
1.87	1.88	030

the second phase was of large cell (~ 4 Å). On a qualitative basis the proportion of the second phase increased with increased substitution of Sc ions.

The composition corresponding to $La(Al_{0.8}Sc_{0.2})O_3$ after sintering in Experiment #12 was used as meltstock in Experiment #14. With sintered meltstock the volatilization of charge is minimized. Single phase material of rhombohedral symmetry with a lattice parameter of 3.86Å was obtained. This data shows that Sc can be incorporated in $LaAlO_3$ and enlarge the lattice but will not change the symmetry to cubic. The crystals showed orange in the fluorescence spectra. This may be because Ce^{3+} is expected to show light green and Ce^{4+} yellow fluorescence. The high concentration of dopant used may have converted some of the Ce to the tetravalent state. The concentration of the dopant was reduced in the charge from 1% to 0.05%.

When material corresponding to $La(Al_{0.5}Sc_{0.5})O_3$ was melted and directionally solidified by HEM in Experiment #15, two phases were observed in the structure, and the x-ray pattern was similar to the solid-state synthesized material of the same composition. This suggested that for Sc concentration between 20 and 50%, a transition in structure may be possible. Therefore, a sample corresponding to $La(Al_{0.75}Sc_{0.25})O_3$ composition was melted and directionally solidified by HEM in Experiment #17. X-ray diffraction data on this sample showed a single phase cubic structure with a unit cell size of 3.83 Å. The data is shown in Table IV.

Thin sections cut out of the solidified material from Experiment #19 corresponding to $La(Al_{0.75}Sc_{0.25})O_3$ composition and lower dopant concentration showed translucency in the as-cut sections. Samples were sent to ONR for evaluation. It was seen that a blue fluorescence was observed in localized areas of a sample which was attributed to color centers in the sample. Another feature observed was that significant carbon contamination was observed in the samples. This contamination masked the structural as well as the optical properties. The

TABLE IV. X-ray diffraction data on sample corresponding to $La(Al_{0.75}Sc_{0.25})O_3$ composition (a=3.832 Å)

Intensity	d_{obs}	d_{calc}	hkl
52	3.84	3.832	100
100	2.72	2.710	110
44	2.22	2.212	111
62	1.92	1.916	200
18	1.71	1.714	210
34	1.57	1.564	211
12	1.35	1.355	220
12	1.28	1.277	300,221
12	1.21	1.212	310
7	1.159	1.155	311
4	1.109	1.1062	222
4	1.063	1.0628	320
10	1.025	1.0241	321
4	0.955	0.9580	400
3	0.927	0.9294	410,322
5	0.900	0.9032	411,330
3	0.879	0.8791	331
5	0.855	0.8569	420
2	0.832	0.8362	421

source of carbon is from the graphite resistance furnace and is being transported via the vapor phase to the charge. Efforts were made to improve the quality of the $La(Al_{0.75}Sc_{0.25})O_3$ crystals in Experiments 20 through 23. These samples exhibited a range of fluorescence from orange to bluish white. The orange is associated with Ce^{4+} and blue to a combination of Ce^{4+} and color centers.

Two experiments (#26 and #27) were carried out to minimize the carbon transport. An extension tube was added to the crucible as shown in Figure 5. The charge after meltdown and solidification still showed carbon contamination. In the second experiment the extension tube was extended further to just below the viewport, but carbon contamination was still observed. At a temperature of ~ 2100°C, carbon contamination from a graphite heat zone is a serious problem. Refractory metal furnaces eliminate the carbon problems. However, they are designed to operate under vacuum, but for $LaAlO_3$ type compounds, it is necessary to operate under pressure to prevent volatilization of charge.

While simple perovskites usually show deviations from cubic symmetry, it is also possible to achieve cubic structure by ordering of ions. Based upon the tolerance factor and ionic sizes of A and B ions a composition corresponding to $La(Al_{0.33}Sc_{0.67})O_3$ was selected to evaluate whether cubic symmetry is achievable by ordering of Al and Sc ions. Experiments #30 through #33 were carried out using this composition. X-ray analysis showed that the major phase was orthorhombic with lattice parameters of a=5.61 Å, b=5.67 Å and c=8.02 Å with a minor phase which was cubic with a lattice parameter of 3.85 Å. These data are consistent with the cubic lattice parameter obtained with $La(Al_{0.75}Sc_{0.25})O_3$ composition.

The rhombohedral structure of $LaAlO_3$ can be enlarged with the addition of Sc in the lattice based on the data obtained for the $La(Al_{1-x}Sc_x)O_3$ system. The enlargement of the structure reduces the deviations from ideal perovskite structure. At

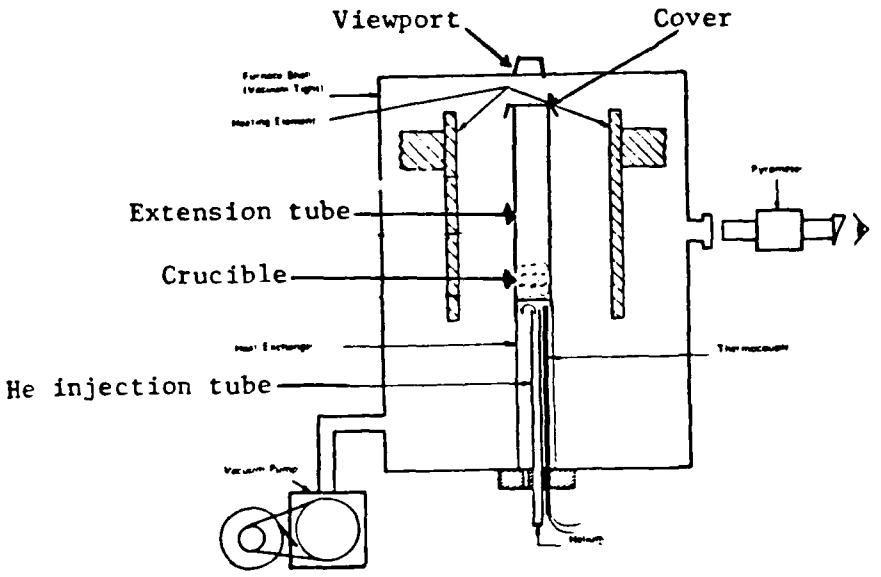

Figure 5. Experimental set-up to prevent carbon contamination

approximate value of x=0.25, single phase cubic structure can be obtained. For higher values of x, the structure changes to orthorhombic and continues to enlarge in cell size until all the Al is replaced by the Sc ions.

For an approximate composition of $La(Al_{0.75}Sc_{0.25})O_3$ single phase cubic material can be produced; however, the composition range is narrow. These crystals should not exhibit twinning like the $LaAlO_3$ composition because of absence of phase transitions. Although single crystals were grown, the fluorescence spectra showed problems with color centers. The quality of the crystals could not be improved because of carbon contamination from the existing furnaces. Crystal growth at about 2100°C under argon atmosphere is very difficult with commercially available refractory metal furnaces.

3.2 Achievement of Cubic Symmetry in Other Perovskites.

After an initial emphasis on the $Ce:La(Al,Sc)O_3$ system described above, efforts were made to identify other perovskite oxides which could lead to a cubic symmetry. If cubic symmetry is achieved at room temperature, then phase transitions will be eliminated. With such materials, single crystal growth can be carried out and twinning and cracking problems will not be encountered. A number of mixed oxide perovskites were evaluated using this approach.

3.2.1 Correlation of Ionic Size and Tolerance Factor

$LaAlO_3$ exhibits a typical ABO_3 type perovskite structure. While none of the $A^{3+}B^{3+}O_3$ type compounds have the "ideal" cubic perovskite structure, the rhombohedral form of $LaAlO_3$ is only a slight distortion from the cubic structure. Partial substitutions of A and/or B ions in some perovskite compounds have led to the formation of cubic structures. For example, $LaCoO_3$ exhibits a rhombohedral structure[22,23]; however, $La_{0.5}Sr_{0.5}CoO_3$ shows a cubic structure[24,25]. Similarly, $BaCeO_3$ is orthorhombic[26], but $BaCe_{0.5}U_{0.5}O_3$ is cubic[27]. Substituted

perovskites usually show ordering of the A and/or B ions and lead to the formation of a larger unit cell size with a cubic structure.

Ordering of the ions takes place when there is a large difference in their charge or size. The range of ionic size that can form the perovskite structure is governed by the Goldschmidt tolerance factor, t. This factor for oxides is given by

$$t = (R_A + R_O)/\sqrt{2}\,(R_B + R_O)$$

where R_A, R_B and R_O are the radii of the A, B and oxygen ions, respectively. The perovskite structure is stable within the range of $0.75 < t < 1.00$ with t lying between 0.8 and 0.9 in most cases.

Using $LaAlO_3$ as a host lattice and partial substitution of Al with Sc, the tolerance factor for $La(Al_{1-x}Sc_x)O_3$ changes from 0.9302 for $x = 0$ to 0.8167 for $x = 1$. The experimental work described above shows that for this system, when $x = 0.25$, a cubic structure may be formed. For this compound $t = 0.8990$.

Other suitable substitutions for La and Al are Gd and Ga, respectively. Literature values of the ionic radii of different ions are shown in Table V. Tolerance factor calculations for various systems with substitution for La or Al, as well as both La and Al, are shown in Table VI. It can be seen that the four systems indicated show a wide range of t values with all values being in the range of Goldschmidt criterion for formation of perovskite structure.

The cubic structure is formed because of ordering when there is a difference in valence or ionic size. In the systems discussed, ordering because of valence difference is not expected because all cations are trivalent. The difference in ionic sizes to achieve ordering for the $A^{3+}B^{3+}O_3$ system is not known; however, a study[12] of $Ba(M^{3+}_{0.5}Nb^{5+}_{0.5})O_3$ type compounds showed that the critical percentage difference in ionic radii between B ions which causes ordering lies between 7% and 17%. Calculations for La, Gd and Al,Ga systems show that the percentage difference in ionic radii is 17.5 and 12.7%, respectively.

TABLE V. Literature values of ionic radii for A^{3+} and B^{3+} ions

Atom	Ionic Radius, Å
La	1.14
Gd	0.97
Sc	0.81
Ga	0.62
Al	0.55
O^{2-}	1.32

TABLE VI. Tolerance factor, t, calculations of various perovskite structures using ionic radii in Table II.

System	tolerance factor, t		
	x=0 y=0	x=0.5 y=0.5	x=1.0 y=1.0
$La(Al_{1-x}Sc_x)O_3$	0.9302	0.8697	0.8167
$La(Al_{1-x}Ga_x)O_3$	0.9302	0.9131	0.8966
$(La_{1-y}Gd_y)AlO_3$	0.9302	0.898	0.8659
$(La_{1-y}Gd_y)(Al_{1-x}Ga_x)O_3$	0.9302	0.8816	0.8347

Another advantage of these substituted compounds is that they are expected to have lower melting points. This will facilitate crystal growth and make it easier to retain Ce dopant in the trivalent state necessary for blue-green luminescence. This approach utilizes only trivalent ions and tends to facilitate keeping Ce in trivalent state.

Another approach is to utilize partial replacement of A ions with divalent ions and B ions with tetravalent ions. With this approach ordering may be achieved by differences in ionic sizes as well as charges on the ions. It may also be possible to obtain cubic symmetry without the ordering when multi-valent ions are used. For these purposes, mixtures of $A^{3+}B^{3+}O_3$ with $BaZrO_3$ and $SrZrO_3$ were evaluated because these ions do not exhibit multi-valence state and therefore are not expected to form Ce^{4+} state for the dopant.

3.2.2 Crystal Growth of Other Perovskite Compounds by HEM

In Experiments #34 through #36 achievement of cubic structure by ordering of A ions in the composition $(La_{1-x}Gd_x)ScO_3$ system with x = 0.25 and 0.5 was investigated. The cubic phase was not obtained and the major phase was identified as orthorhombic with lattice parameter of a = 5.766, b = 7.980 and c = 5.523 Å for #34.

Composition $Gd(Al_{0.5}Sc_{0.5})O_3$ in Experiment #38 also did not yield the cubic phase. Ga substitution in the B site was not attempted because of the formation of Ga_2O under reducing conditions and problems with maintaining stoichiometry.

In Experiments #37 and #40, a 50:50 mixture of $BaZrO_3$ with $LaScO_3$ and $LaAlO_3$, respectively, were attempted. In both cases, cubic enlarged cell expected from ordering was not observed. Similar results were achieved in Experiment #47 with $(LaAlO_3)_{0.5}(SrZrO_3)_{0.5}$ composition.

Small additions of $BaZrO_3$ to $LaAlO_3$ were evaluated for $(LaAlO_3)_{1-x}(BaZrO_3)_x$ for x = 0.02 and 0.05 in Experiments #39, #42, and #46. It was observed that for x = 0.05, the major phase

was cubic, and for x = 0.02, nearly all the material showed cubic structure with a_o = 3.81Å. Traces of $La(OH)_3$ were also observed in the x-ray pattern. Similar results were also achieved when $SrZrO_3$ was added to $LaAlO_3$. The bluish-green crystals grown are not expected to exhibit blue-green fluorescence. Ce:$BaZrO_3$ did not exhibit any fluorescence.

The results of investigations of other perovskites have shown that in the compositions evaluated, enlarged cubic cells could not be formed by ordering. Small additions of less than 5% of $BaZrO_3$ or $SrZrO_3$ to $LaAlO_3$ produced cubic symmetry which should allow growth of twin-free crystals. The crystals grown did not exhibit blue-green fluorescence.

3.3 Evaluation of Low Melting Point Hosts

$LaAlO_3$ appears to be an appropriate host for Ce^{3+} for blue-green laser applications. However, because of phase transitions, twin-free crystals cannot be grown. Suitable additions to $LaAlO_3$ can be made to transform the structure to cubic phase which will eliminate the phase transitions. However, the crystal growth conditions required cannot be easily achieved with available equipment. An evaluation was made of lower melting point host materials which could be grown as single crystals.

For these purposes, efforts were made to grow Ce-doped crystals of Gd_2SiO_5 and La_2SiO_5. These samples were sent to ONR for fluorescence measurements toward the end of the experimental program, but data was not obtained.

A sample of Pr:$KMgY_3F_{12}$ obtained from Airtron was also directionally solidified by HEM and sample sent to ONR.

Recent interest in Cr,Nd:$Gd_3Sc_2Al_3O_{12}$ (GSAG) laser crystals prompted interest in evaluation of Ce:GSAG crystals. Yellow crystals approximately cm size were grown by HEM and evaluated at the Naval Research Laboratory. It was observed[28] that emission varied with the pump wavelength. Three fluorescence peaks centered at 380, 485, and 795 nm were observed. The fluorescence spectra of Ce:GSAG with an excitation at 365 nm is shown in

Figure 6. While this material showed interesting results, the fluorescence data was received after the end of the experimental program. In order to further evaluate the laser performance of this crystal, it would be necessary to grow improved quality crystals using higher purity starting materials.

Figure 6.

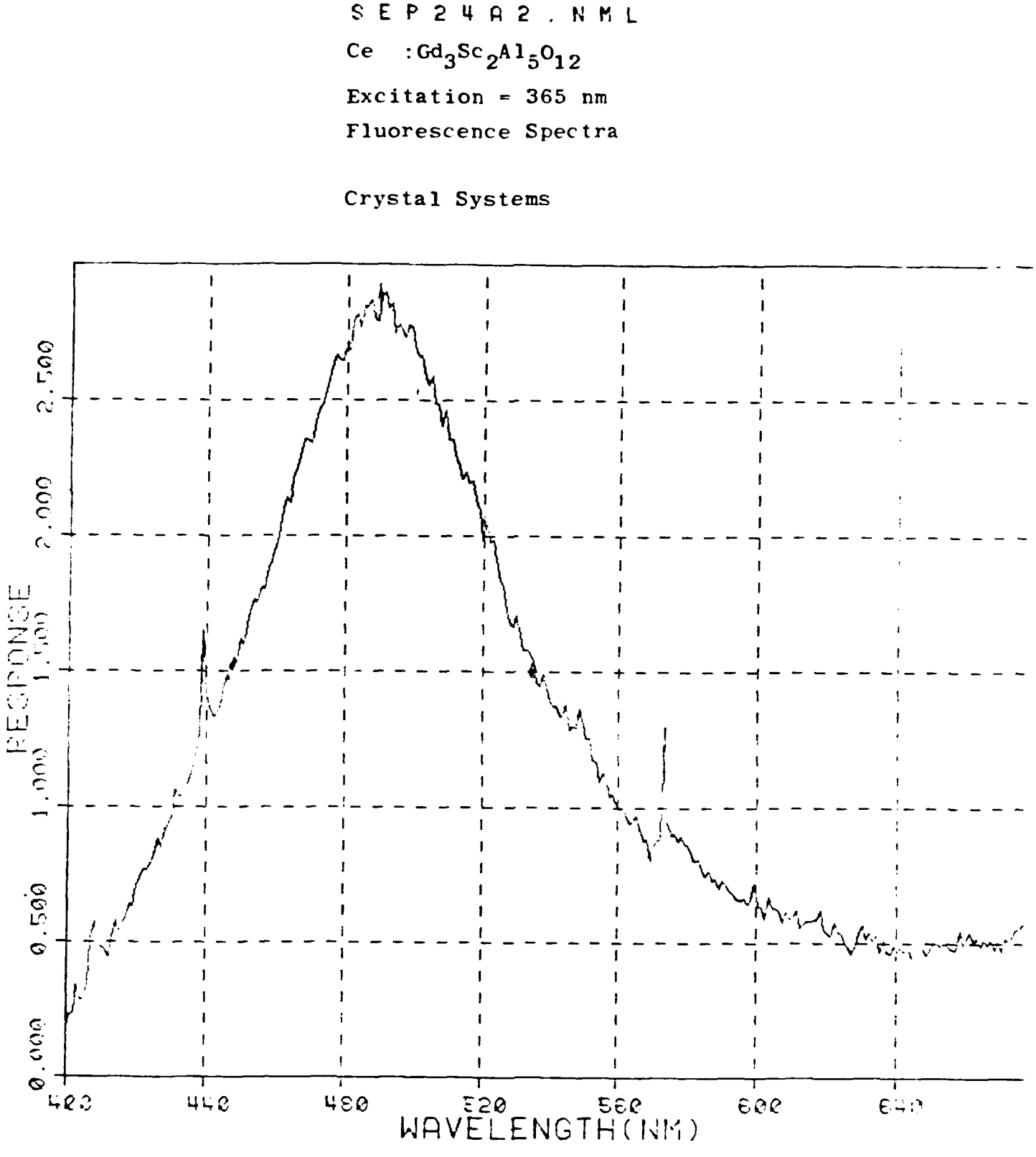
SEP24A2.NML
Ce :$Gd_3Sc_2Al_5O_{12}$
Excitation = 365 nm
Fluorescence Spectra
Crystal Systems
RESPONSE
0.000
0.500
1.000
2.000
2.500
400
440
480
520
560
600
640
WAVELENGTH(NM)

4.0 Conclusions

Ce:$LaAlO_3$ offers promise as a solid state laser crystal for communication under seawater. The phase transition at 435° C for $LaAlO_3$ does not allow growth of high quality crystals. Initial emphasis of the program was on making suitable additions to the $LaAlO_3$ in order to achieve a cubic perovskite structure which eliminates the phase transition. A composition of $La(Al_{0.75}Sc_{0.25})O_3$ was identified as cubic; however, high quality crystals could not be grown because of difficult crystal growth parameters which could not be obtained with available equipment. Two other compositions - $(La_{0.98}Ba_{0.02})(Al_{0.98}Zr_{0\ 02})O_3$ and $(La_{0.98}Sr_{0.02})(Al_{0.98}Zr_{0.02})O_3$ - were also produced with cubic structure. Since Ba containing compound may exhibit quenching of fluorescence, the Sr compound may be useful for solid state laser applications. These bluish-green crystals are not expected to show fluorescence in the blue-green spectral region.

In order to develop other crystals with lower melting point, an effort was also placed on Ce:Gd_2SiO_5, Ce:La_2SiO_5 and Pr:$KMgY_3F_{12}$. These samples were delivered to ONR for evaluation of fluorescence.

Ce:$Gd_3Sc_2Al_3O_{12}$ (Ce:GSAG) crystals were also grown by HEM. These crystals offer promise for solid state laser applications; however, it is necessary to grow improved quality crystals for evaluation of laser performance.

5.0 References

1. G. Blasse and A. Bril, Appl. Phys. Letters II, 53 (1967).
2. G. Blasse and A. Bril, J. Chem. Phys. 47, 5139 (1967).
3. M. J. Weber, Rare Earth Lasers in: K.A. Gschneidner, Jr., and L. Eyring, eds., Rare Earths (North Holland Publ. Co., NY) Vol. 4, p. 275 (1979).
4. W. Miniscalco, J. Pellegrino and W. Yen, J. Appl. Phys. 49, 6109 (1978).
5. B. Derighetti, J. E. Drumheller, F. Laves, K. A. Muller and F. Waldner, Acta Crystallogo. 18, 557 (1965).
6. V. O. Nicolai, Office of Naval Research, private communication.
7. F. Schmid and C. P. Khattak, Laser Focus/Electro-Optics 19 (9), 147 (1983).
8. C. P. Khattak and F. Schmid, Proc. SPIE Conf. on Advances in Optical Materials (S. Musikant ed.) 505, 4 (1984).
9. F. Schmid and C. P. Khattak, Springer Series in Optical Sciences (P. Hammerling, A. B. Budgor and A. Pinto eds.) 47, 122 (1985).
10. C. P. Khattak and A. N. Scoville, Proc. SPIE's International Tech. Symp. San Diego, CA, Ang. 1986 (in press).
11. S. Geller and V. B. Bala, Acta Crystallogr. 9, 1019 (1956).
12. F. S. Galasso, International Series of Monographs in Solid State Physics (Pergamon Press, New York) 5 (1969).
13. D. H. Templeton and C. H. Bauben, J. Amer. Chem. Soc. 76, 5237 (1954).
14. W. H. Zachariasen, Crystal Chemistry of 5f Elements: in G. T. Seaborg and J. J. Katz, eds., The Actinide Elements (McGraw Hill Book Co., NY) p. 769 (1954).
15. C. P. Khattak and F. F. Y. Wang, Perovskites and Garnets: in Handbook on the Physics and Chemistry of Rare Earths, K. A. Gschneidner, Jr., and L. Eyring eds. (North Holland Publ. Co., NY) Vol. 3 p. 525 (1979).
16. S. Geller, Acta Crystallogr. 10, 243 (1957).

17. J. A. Bondar and N. V. Vinogradova, Izv. Akad. Nauk SSSR, Ser. Khim., No. 5, 785 (1964).
18. N. A. Toropov and V. A. Vasil'eva, Dokl. Akad. Nauk SSSR, 152, 1379 (1963).
19. R. S. Roth, J. Res. NBS 58, 75 (1957).
20. M. L. Keith and R. Roy, Am. Mineral 39, 1 (1954).
21. M. Mizuno et al, Yagyo-Kyokai-Shi 82, 631 (1974).
22. A. Wold, B. Post and E. Banks, J. Amer. Ceram. Soc. 79, 6365 (1957).
23. P. M. Raccah and J. B. Goodenough, Phys. Rev. 155, 932 (1967).
24. H. L. Yakel, Jr., Acta Crystallogr. 8, 394 (1955).
25. P. L. Gai and C. N. R. Rao, Mater. Res. Bull. 10, 787 (1975).
26. A. J. Jacobson, B. C. Toefield and B.E.F. Fender, Acta Crystallogr. B28, 956 (1972).
27. S. K. Awasthi, D. M. Chakraburtty and V. K. Tandon, J. Inorg. Nucl. Chem. 29, 1225 (1967).
28. L. Esterowitz, Naval Research Laboratory, personal communication.

END

3-87

DTIC